5

Walking Support and Power Assistance of a Wheelchair Typed Omnidirectional Mobile Robot with Admittance Control

Chi Zhu[1], Masashi Oda[1], Haoyong Yu[2], Hideomi Watanabe[3] and Yuling Yan[4]

[1]*Department of Systems Life Engineering, Maebashi Institute of Technology, Kamisadori 460-1, Maebashi, Gunma, 371-0816.*

[2]*Bioengineering Division, Faculty of Engineering, National University of Singapore*

[3]*Department of Health Sciences, Faculty of Medicine, Gunma University*

[4]*School of Engineering, Santa Clara University, CA*

[1,3]*Japan*

[2]*Singapore*

[4]*USA*

1. Introduction

Walking ability is essential for the elderly/the disabled's self-supported daily life. Currently the development of various robotic aids or devices for helping the elderly's walking has attracted many researcher's attentions. Guidecane ((Ulrich & Borenstein, 2001)), PAM-AID ((Lacey & Dawson-Howe, 1998)), Care-O-bot ((Graf et al., 2004)), PAMM ((S. Dubowsky, 2000)), and etc, are developed for intelligent walking support and other tasks for the elderly or the disabled. Mainly for the elderly's walking support, a robotic power-assisted walking support system is developed (Nemoto & M. Fujie, 1998). The system is to support the elderly needing help in standing up from the bed, walking around, sitting down for rehabilitation.

Meanwhile, a number of intelligent wheelchair-type aids are being designed for people who cannot walk and have extremely poor dexterity ((Yanco, 1998)-(Dicianno et al., 2007)). These devices are well suited for people who have little or no mobility, but they are not appropriate for the elderly with significant cognitive problems. Consequently, the facilities are generally reluctant to permit the elderly residents to use powered wheelchairs. Hence, the better solution is that the facility staff (the caregiver) pushes the wheelchair to move. Some technologies for the caregiver's power assistance are proposed ((Kakimoto et al., 1997)-(Miyata et al., 2008)).

Further, since the omnidirectional mobility is necessary to truly yield the user's (here refer to the elderly/disabled, or the caregiver) intentions of walking speed and direction, omnidirectional mobility is investigated in order to obtain a smooth motion and high payload capability, not with the special tires but with the conventional rubber or pneumatic tires. An omnidirectional and holonomic vehicle with two offset steered driving wheels and two

free casters is proposed (Wada & Mori, 1996). An omnidirectional mobile robot platform using active dual-wheel caster mechanisms is developed (Han et al., 2000), in which, the kinematic model of the active dual-wheel caster mechanism is derived and a holonomic and omnidirectional motion of the mobile robot using two such assembly mechanisms is realized. An omnidirectional platform and vehicle design using active split offset casters (ASOC) is also developed (Yu et al., 2004). Its structure is very similar to (Han et al., 2000), but particular attention is paid to the system performance on uneven floors.
However, up to now, the wheelchair typed robot that can be used either for the elderly's walking support, or the disabled's walking rehabilitation, or the caregiver's power assistance has not been reported yet. In this study, we develop such kind of wheelchair typed omnidirectional robot that not only can support the elderly or the disabled's walking, but also can lessen the caregivers' burden, or saying, give the caregivers power assistance.

2. Overview of the developed robot

The developed new type of omnidirectional mobile robot for the elderly's walking support, the disabled's rehabilitation, and the caregiver's power assistance, is shown in Fig. 1. Its structure is illustrated in Fig. 2.

Fig. 1. The omnidirectional mobile robot in developing for the elderly's walking support, the disabled's walking rehabilitation, and the caregiver's power assistance

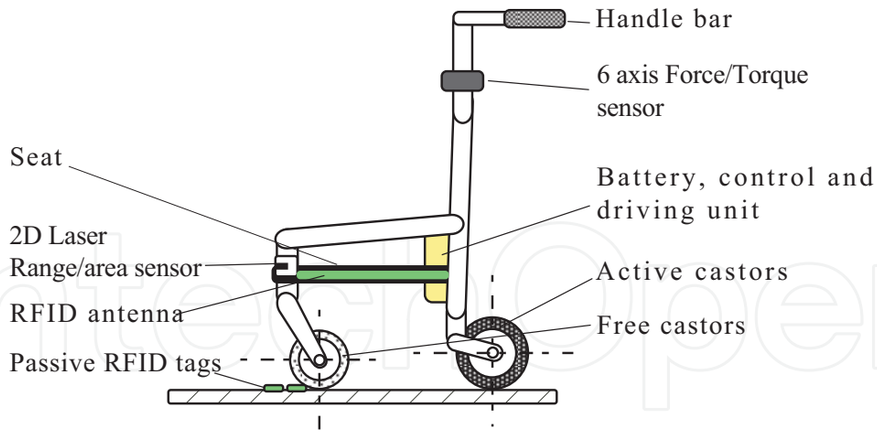

Fig. 2. The structure of the robot

2.1 The robot objective and functions

Different from the other intelligent aids, the robot has a handle and a seat. The user holds the handle with his/her hands during walking. Usually, the elderly's walking ability (the capable walking distance), can be greatly enhanced with the help of the intelligent walking support devices. However, because of the muscle weakness, the knee and waist of the elderly will be painful after walking some distances. At that time, the elderly hopes to have a seat for a rest. To meet such a very actual requirement, we embed a seat in the robot so that the elderly or the disabled can take a seat for rest when necessary. On the other hand, when the elderly or the disabled is sitting in the seat of the wheelchair type aids and wants to go to somewhere, the caregiver will have to push the wheelchair. Hence, the power assistance of the health caregivers is also necessary.

Consequently, the main the objectives of the robot are To meet the above two main objectives, the functions the robot should have:

1. omnidirectional mobility.
2. few load feeling when the user (the elderly/disabled /caregiver) holding the handle during walking or pushing the robot.
3. guidance to destinations and obstacle avoidance via sensors and pre-determined maps.
4. adaptation to the different motion abilities of the different users.

2.2 Robot structure

The robot shown in Fig.1, 2 is considered to be used either indoor or outdoor. It includes two active dual-wheel modules and two free casters that provides the robot omnidirectional mobility. It will be discussed in section 3 in detail.

A 6-axis force/torque sensor, mounted on the shaft of the handle, detects the forces and torques the user applies to the handle. With these force/torque signals, the embedded computer estimates the user's intention of walking velocity and walking direction, and the robot is controlled to yield the user's intention so that the user will feel few loads to fulfill the walking support and power assistance. The detail will be explained in section 4.

The 2D laser ranger/area finder is employed to detect the obstacles. The RFID system of the RFID antenna under the seat and the passive RFID tags laid under or near the places such as

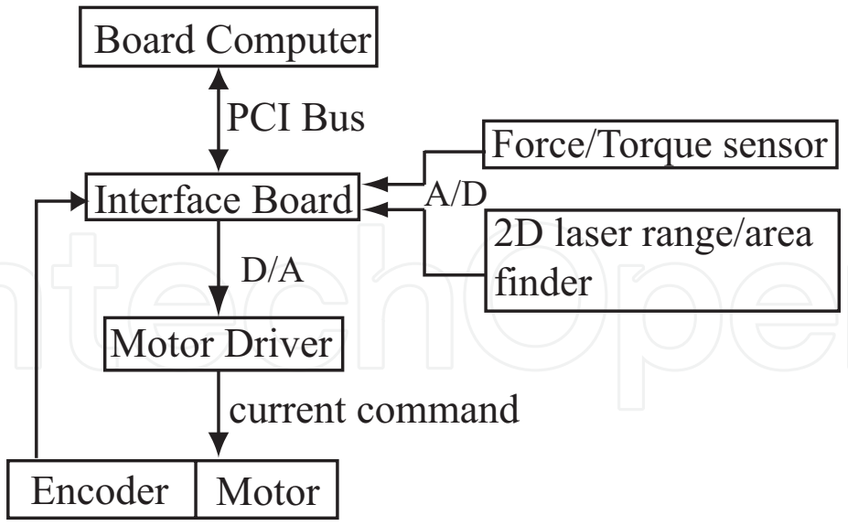

Fig. 3. The control system of the robot

the door, corner, elevator are used to identify the robot position and orientation. They are used for the destination guidance and obstacle avoidance. The problems of such obstacle avoidance and navigation are not discussed in this chapter.
The control system of the robot as shown in Fig. 3 consists of a board computer running RTLinux operation system, an multi-functional interface board, two motor drivers in which each motor driver can drive two motors.

3. Omnidirectional mobility

The wheels of the robot consists of two active dual-wheel modules and two free casters. The two active dual-wheel modules enable the robot omnidirectional mobility and the two free casters keep the robot balance. First we analyze the kinematics of one dual-wheel module, than investigate the omnidirectional mobility of the robot realized by two dual-wheel modules.

3.1 Kinematics of one dual-wheel module

As shown in Fig. 4, an active dual-wheel module consists of two independently driven coaxial wheels, which are separated at a distance $2d$ and connected via an offset link s to the robot at the joint O_i. The coordinate systems, valuables, and parameters are defined as follows.
$O_wX_wY_w$: a world coordinate system.
$O_iX_iY_i$: a moving coordinate system attached to the wheel module i at the offset link joint O_i.
x_i, y_i: coordinates of the origin O_i of the frame $O_iX_iY_i$ with respect to the ground (the frame $O_wX_wY_w$). Consequently, their derivations to time
$\dot{x}_i, \dot{y}_i$: velocities of the joint O_i respectively in the X_i, Y_i axes.
$\dot{x}_{wi}, \dot{y}_{wi}$: velocities of the joint O_i respectively in the X_w, Y_w axes.
ϕ_i: orientation of the module i with respect to the world frame.
$\boldsymbol{u_i}, \boldsymbol{u_{wi}}$: velocity vectors of the joint O_i respectively with respect to the frame $O_iX_iY_i$ and ground $O_wX_wY_w$, where, $\boldsymbol{u_i} = [\dot{x}_i, \dot{y}_i]^T$ and $\boldsymbol{u_{wi}} = [\dot{x}_{wi}, \dot{y}_{wi}]^T$.
ω_{li}, ω_{ri}: respectively the left and right wheel's angular velocities of the module i.

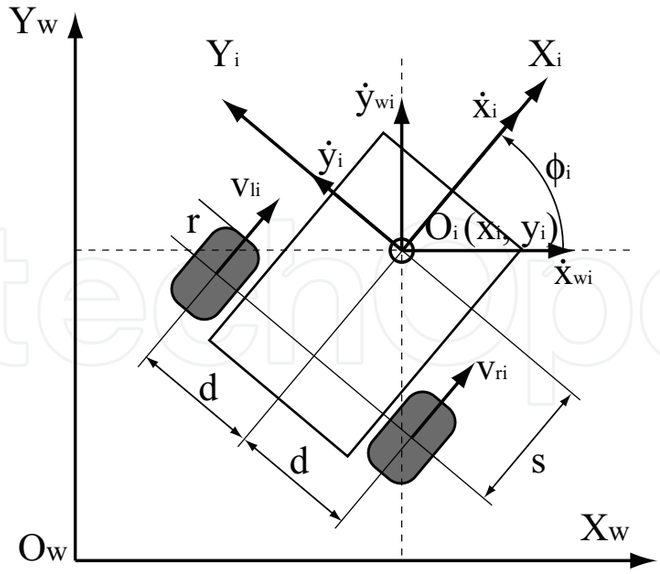

Fig. 4. Model of one active dual-wheel module

$\boldsymbol{\omega_i}$: angular velocity vector of the module i. $\boldsymbol{\omega_i} = [\omega_{li}, \omega_{ri}]^T$.
r: radius of the wheels.
The linear velocities of the joint O_i of the module i can be expressed as:

$$\boldsymbol{u_i} = \begin{bmatrix} \dot{x}_i \\ \dot{y}_i \end{bmatrix} = \frac{r}{2} \begin{bmatrix} 1 & 1 \\ \frac{s}{d} & -\frac{s}{d} \end{bmatrix} \cdot \begin{bmatrix} \omega_{ri} \\ \omega_{li} \end{bmatrix} = \boldsymbol{J_i} \cdot \boldsymbol{\omega_i} \tag{1}$$

where $\boldsymbol{J_i}$ is the Jacobian matrix of the module in the moving frame $O_iX_iY_i$.
On the other hand, the velocity of the joint O_i expressed in the world system is given by

$$\boldsymbol{u_{wi}} = \begin{bmatrix} \dot{x}_{wi} \\ \dot{y}_{wi} \end{bmatrix} = \begin{bmatrix} \cos\phi_i & -\sin\phi_i \\ \sin\phi_i & \cos\phi_i \end{bmatrix} \cdot \boldsymbol{u_i} = \boldsymbol{R_i} \cdot \boldsymbol{u_i} \tag{2}$$

Therefore, the kinematics of the module between the velocity of the joint O_i and the two wheel rotation velocities is expressed as:

$$\boldsymbol{u_{wi}} = \boldsymbol{R_i} \cdot \boldsymbol{J_i} \cdot \boldsymbol{\omega_i} = \boldsymbol{J_{wi}} \cdot \boldsymbol{\omega_i} \tag{3}$$

where $\boldsymbol{J_{wi}}$ is the Jacobian matrix of the module in the world frame $O_wX_wY_w$, and it is given as:

$$\boldsymbol{J_{wi}} = \frac{r}{2} \begin{bmatrix} \cos\phi_i - \frac{s}{d}\sin\phi_i & \cos\phi_i + \frac{s}{d}\sin\phi_i \\ \sin\phi_i + \frac{s}{d}\cos\phi_i & \sin\phi_i - \frac{s}{d}\cos\phi_i \end{bmatrix} \tag{4}$$

The above expressions indicate that the velocity of the module is determined by the parameters s, d, r, and ω_{ri}, ω_{li}. But since s, d, r are structurally determined for a robot, the only controllable values are angular velocities ω_{ri}, ω_{li} of the two driving wheels. The determinant of $\boldsymbol{J_{wi}}$ is :

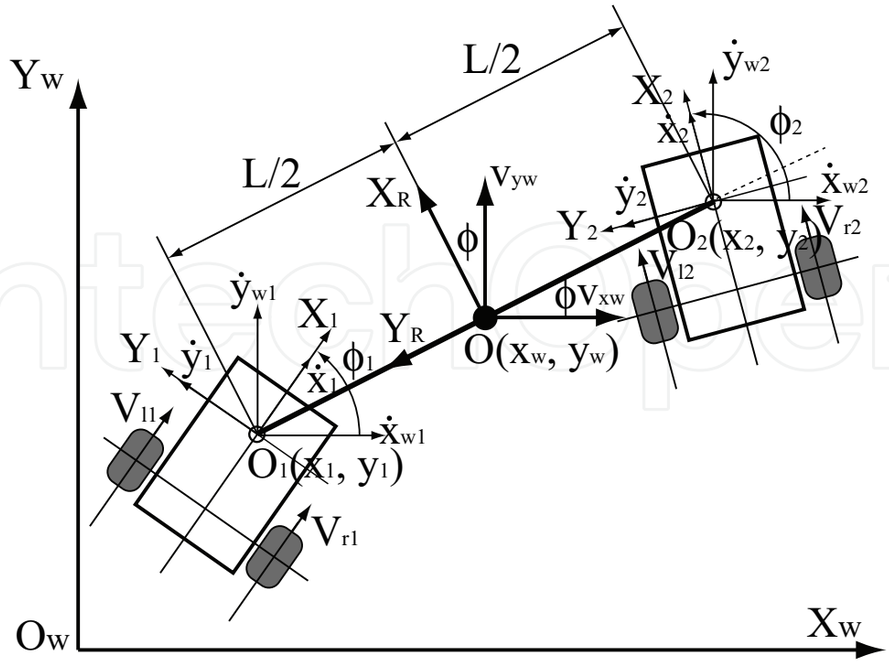

Fig. 5. Model of two active dual-wheel modules

$$\det \mathrm{J}_{wi} = -\frac{\mathrm{r}^2 \mathrm{s}}{2\mathrm{d}} \tag{5}$$

This means that the module has no singularity as long as the distance s is not zero. This fact implies that arbitrary and unique velocities at the joint point O_i can be achieved by appropriately controlling the rotational velocities of the two wheels. Note that one such a module only has 2DOF. In other words, omnidirectional mobility (3DOF) cannot be achieved. Consequently, at least two modules are necessary to realize omnidirectional mobility. In this study, two modules are used to achieve the omnidirectional mobility.

3.2 Omnidirectional mobility with two modules

As shown in Fig.5, two active dual-wheel modules consists of a basic part of the mobile robot that enable the robot to have omnidirectional mobility.

In Fig. 5, point O is the center of the robot platform. Its coordinates and velocities in the world frame $O_w X_w Y_w$ are respectively (x_w, y_w) and (v_{xw}, v_{yw}). The frame $OX_R Y_R$ is attached to the robot. ϕ is the orientation of the robot. The vector $\boldsymbol{V} = [v_{xw}, v_{yw}, \dot{\phi}]^T$ is the velocity vector of the robot. The distance between the two joint points of two modules is L. $\boldsymbol{\omega} = [\omega_{r1}, \omega_{l1}, \omega_{r2}, \omega_{l2}]^T$ is the angular velocity vector of the four driving wheels of the robot.

To obtain the rotational velocity $\dot{\phi}$ of the robot, it it convenient to transform $\dot{x}_{wi}, \dot{y}_{wi}$ in the world frame to the robot frame $OX_R Y_R$. The relationship is given by

$$\begin{bmatrix} \dot{x}_{Ri} \\ \dot{y}_{Ri} \end{bmatrix} = \begin{bmatrix} \cos\phi & -\sin\phi \\ \sin\phi & \cos\phi \end{bmatrix} \cdot \begin{bmatrix} \dot{x}_{wi} \\ \dot{y}_{wi} \end{bmatrix} \tag{6}$$

Therefore, $\dot{\phi}$ of the robot can be expressed as

$$\dot{\phi} = \frac{\dot{x}_{R2} - \dot{x}_{R1}}{L} \tag{7}$$

$$= \frac{1}{L}\left[(\dot{x}_{w2} - \dot{x}_{w1})\cos\phi + (\dot{y}_{w2} - \dot{y}_{w1})\sin\phi\right] \tag{8}$$

Hence, the velocity vector $\boldsymbol{V}$ can be expressed as:

$$\boldsymbol{V} = \begin{bmatrix} v_{xw} \\ v_{yw} \\ \dot{\phi} \end{bmatrix} = \frac{1}{2}\begin{bmatrix} 1 & 0 & 1 & 0 \\ 0 & 1 & 0 & 1 \\ -\frac{\cos\phi}{L} & -\frac{\sin\phi}{L} & \frac{\cos\phi}{L} & \frac{\sin\phi}{L} \end{bmatrix} \cdot \begin{bmatrix} \dot{x}_{w1} \\ \dot{y}_{w1} \\ \dot{x}_{w2} \\ \dot{y}_{w2} \end{bmatrix} \tag{9}$$

From (3), the velocity vector $[\dot{x}_{w1}, \dot{y}_{w1}, \dot{x}_{w2}, \dot{y}_{w2}]^T$ in the above expression is given by

$$\begin{bmatrix} \dot{x}_{w1} \\ \dot{y}_{w1} \\ \dot{x}_{w2} \\ \dot{y}_{w2} \end{bmatrix} = \frac{r}{2}\begin{bmatrix} \boldsymbol{A_1} & \boldsymbol{0_{2\times 2}} \\ \boldsymbol{0_{2\times 2}} & \boldsymbol{A_2} \end{bmatrix} \cdot \begin{bmatrix} \omega_{r1} \\ \omega_{l1} \\ \omega_{r2} \\ \omega_{l2} \end{bmatrix} = \boldsymbol{A} \cdot \begin{bmatrix} \omega_{r1} \\ \omega_{l1} \\ \omega_{r2} \\ \omega_{l2} \end{bmatrix} \tag{10}$$

where

$$\boldsymbol{A_i} = \begin{bmatrix} \cos\phi_i - \frac{s}{d}\sin\phi_i & \cos\phi_i + \frac{s}{d}\sin\phi_i \\ \sin\phi_i + \frac{s}{d}\cos\phi_i & \sin\phi_i - \frac{s}{d}\cos\phi_i \end{bmatrix} \tag{11}$$

Furthermore, the robot possessing omnidirectional mobility realized by two active dual-wheel modules has three degrees of freedom with a total of four actuators. There should be a constraint for this redundancy. The physically constant distance between the two joint points O_1 and O_2 is used to eliminate the redundancy. It leads the following velocity constraint:

$$\dot{y}_{R1} = \dot{y}_{R2} \tag{12}$$

From (6) it means

$$0 = \dot{x}_{w1}\sin\phi - \dot{y}_{w1}\cos\phi - \dot{x}_{w2}\sin\phi + \dot{y}_{w2}\cos\phi \tag{13}$$

By combining Eqs. (9), (10) and (13), we can get the following homogeneous forward kinematics of the robot:

$$\begin{bmatrix} \boldsymbol{V} \\ 0 \end{bmatrix} = \begin{bmatrix} v_{xw} \\ v_{yw} \\ \dot{\phi} \\ 0 \end{bmatrix} = \frac{1}{2}\begin{bmatrix} 1 & 0 & 1 & 0 \\ 0 & 1 & 0 & 1 \\ -\frac{\cos\phi}{L} & -\frac{\sin\phi}{L} & \frac{\cos\phi}{L} & \frac{\sin\phi}{L} \\ \sin\phi & -\cos\phi & -\sin\phi & \cos\phi \end{bmatrix} \cdot \begin{bmatrix} \dot{x}_{w1} \\ \dot{y}_{w1} \\ \dot{x}_{w2} \\ \dot{y}_{w2} \end{bmatrix}$$

$$= \boldsymbol{B} \cdot \begin{bmatrix} \dot{x}_{w1} \\ \dot{y}_{w1} \\ \dot{x}_{w2} \\ \dot{y}_{w2} \end{bmatrix} = \boldsymbol{B} \cdot \boldsymbol{A} \cdot \begin{bmatrix} \omega_{r1} \\ \omega_{l1} \\ \omega_{r2} \\ \omega_{l2} \end{bmatrix} = \boldsymbol{B} \cdot \boldsymbol{A} \cdot \boldsymbol{\omega} \tag{14}$$

Hence, the inverse kinematics of the robot, i.e., with the given desired velocity vector $\boldsymbol{V_d}$ of the robot, the necessary driving velocity vector $\boldsymbol{\omega_d}$ of the four wheels is given by

$$\boldsymbol{\omega_d} = \begin{bmatrix} \omega_{r1} \\ \omega_{l1} \\ \omega_{r2} \\ \omega_{l2} \end{bmatrix} = \boldsymbol{A}^{-1} \cdot \boldsymbol{B}^{-1} \cdot \begin{bmatrix} v_{xw} \\ v_{yw} \\ \dot{\phi} \\ 0 \end{bmatrix} = \boldsymbol{A}^{-1} \cdot \boldsymbol{B}^{-1} \cdot \begin{bmatrix} \boldsymbol{V_d} \\ 0 \end{bmatrix} \tag{15}$$

where,

$$\boldsymbol{A}^{-1} = \frac{1}{r} \begin{bmatrix} \boldsymbol{A_1^{-1}} & \boldsymbol{0} \\ \boldsymbol{0} & \boldsymbol{A_2^{-1}} \end{bmatrix} \tag{16}$$

$$\boldsymbol{A_i^{-1}} = \begin{bmatrix} \cos\phi_i - \frac{d}{s}\sin\phi_i & \sin\phi_i + \frac{d}{s}\cos\phi_i \\ \cos\phi_i + \frac{d}{s}\cos\phi_i & \sin\phi_i - \frac{d}{s}\cos\phi_i \end{bmatrix} \tag{17}$$

$$\boldsymbol{B}^{-1} = \begin{bmatrix} 1 & 0 & -L\cos\phi & \sin\phi \\ 0 & 1 & -L\sin\phi & -\cos\phi \\ 1 & 0 & L\cos\phi & -\sin\phi \\ 0 & 1 & L\sin\phi & \cos\phi \end{bmatrix} \tag{18}$$

Now by rewriting $\boldsymbol{B}^{-1}$ as:

$$\boldsymbol{B}^{*} = \begin{bmatrix} 1 & 0 & -L\cos\phi \\ 0 & 1 & -L\sin\phi \\ 1 & 0 & L\cos\phi \\ 0 & 1 & L\sin\phi \end{bmatrix} \tag{19}$$

We can get the following inverse kinematic equation of the robot:

$$\boldsymbol{\omega_d} = \begin{bmatrix} \omega_{r1} \\ \omega_{l1} \\ \omega_{r2} \\ \omega_{l2} \end{bmatrix} = \boldsymbol{A}^{-1} \cdot \boldsymbol{B}^{*} \cdot \begin{bmatrix} v_{xw} \\ v_{yw} \\ \dot{\phi} \end{bmatrix} = \boldsymbol{A}^{-1} \cdot \boldsymbol{B}^{*} \cdot \boldsymbol{V_d} \tag{20}$$

As discussed in section 4, the $\boldsymbol{V_d}$, the desired velocity of the robot, is obtained from the introduced admittance controller, and the $\boldsymbol{\omega_d}$, each wheel's speed command, is used for velocity control.

4. Admittance based interaction control for power assistance

Admittance of a mechanical system is defined as (Newman (1992))

$$\boldsymbol{G} = \frac{\boldsymbol{V}}{\boldsymbol{F}} \tag{21}$$

where, $\boldsymbol{V}$ is the velocity and $\boldsymbol{F}$ is the contact or applied force, both at the point of interaction. A large admittance corresponds to a rapid motion induced by applied forces; while a small admittance represents a slow reaction to act forces.

Here, admittance controller is introduced in order to fulfill the power assistance when the elderly/disabled holding the handle to walk or the caregiver holding the handle to push the robot while the elderly or the disabled sitting in the seat. Since user's (the elderly, the disabled, or the caregiver) walking speed doesn't change a lot, a large admittance implies relatively small forces needed to exert to the robot. This is the basic principle of power assistance. Note that almost similar approaches had been already used for the elderly's walking support (Nemoto & M. Fujie (1998); Yu et al. (2003)), since our robot can be used both by the elderly/disabled and the caregiver, the approach is extended to the caregiver's power assistance.

In this study, the admittance of the human-robot system can be defined as a transfer function with the user's applied forces and torques, $\boldsymbol{F}(s)$, as input and the robot's velocities, $\boldsymbol{V}(s)$, as the output. The time response $\boldsymbol{V_d}(t)$ of the admittance model is used as the desired velocity of the robot. Then, the desired driving speed $\boldsymbol{\omega_d}$ of each wheel is calculated from $\boldsymbol{V_d}(t)$ by the inverse kinematics equation (20), and the $\boldsymbol{\omega_d}$, as each wheel's speed command, is used for velocity control. The admittance based control process is shown in Fig.6, in which a digital LF (low-pass filter) cuts off the high frequency noises in the force/torque signals from the 6-axis force/torque sensor.

In the forward direction (X_R direction in Fig.5), the admittance can be expressed as

$$G_x(s) = \frac{V_x(s)}{F_x(s)} = \frac{1}{M_x s + D_x} \tag{22}$$

where, M_x and D_x are respectively the virtual mass and virtual damping of the system in forward (X_R) direction.

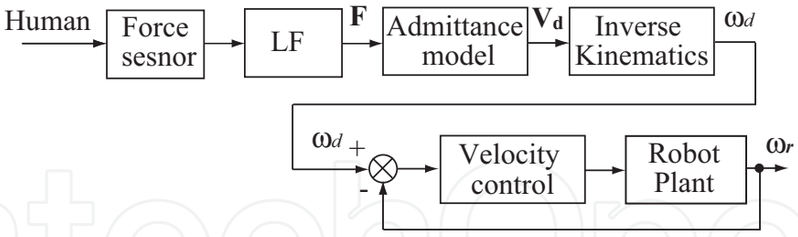

Fig. 6. Admittance based control

The time response $V_{xd}(t)$ for a step input F_x of the above transfer function is:

$$V_{xd}(t) = \frac{F_x}{D_x}(1 - e^{-t/\tau_x}) \tag{23}$$

where, τ_x is the time constant defined by $\tau_x = M_x/D_x$. The steady state velocity of the system is $V_{xs} = F_x/D_x$. This means that the forces to the robot exerted by the user determines the velocities of the system (user and machine). In other words, when the user's steady forward walking velocity is V_{xs} (this velocity usually doesn't change a lot for a user), then the necessary pushing force F_{xs}, or saying, the burden the user feels reacted from the robot, should be

$$F_{xs} = V_{xs} \cdot D_x \tag{24}$$

Fig. 7. A user pushes the robot while a person sitting in the seat.

Thus, by adjusting the virtual damping coefficient D_x, the user will have different burden feeling. And further by altering virtual mass coefficient M_x (therefore τ_x is changed), we can get the different dynamic corresponds of human-machine system. Our experiments will verify this.

5. Experiments and remarks

The omnidirectional mobility of the robot is experimentally implemented in (Zhu et al., 2010). Here, the developed admittance based interaction control is tested. The sampling and control period is 1 [kHz]. As shown in Fig. 7, a user is holding the robot handle to move the robot forward, or lateral, or tuning on the spot while a 65[kg] person sitting in the seat.

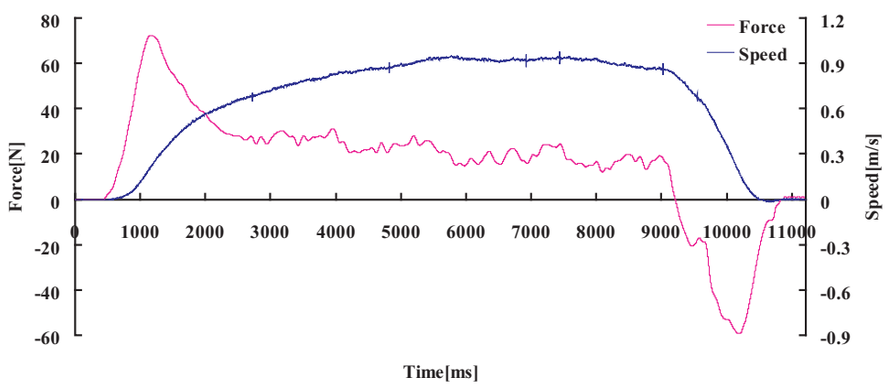

Fig. 8. Forward experimental result without assistance

5.1 Forward experiment without power assistance

First, we turn off the motor drivers and do the experiment without power assistance. In this case, the motors are in free state and the robot is just like a traditional manual-operated wheelchair. From the the result shown in Fig. 8, we can find:

1. to start to move the robot, a big pushing force as large as 70[N] is needed.
2. in steady state, the pushing force is about 24[N].
3. to stop the robot, a negative (pulling) force is needed.
4. the user's walking speed is about 0.9[m/s].

5.2 Forward experiments with power assistance as $D_x = 14$[N·s/m]

In this case, we try to halve the user's burden with power assistance to about 12[N]. Since the user's walking speed is about 0.9[m/s], according to eq.(24) we set $D_x = F_{xs}/V_{xs} = 14$[N·s/m].

Fig. 9 and 10 respectively show the experimental results with $\tau_x = 1.1$[s] ($M_x = \tau_x \cdot D_x = 15.4$[kg]) and $\tau_x = 0.5$[s] ($M_x = 7$[kg]). Both the results show that the pushing force is reduced to about 12[N] from about 24[N] when the steady walking speed is about 0.9[m/s] as we planned, and almost no pulling (negative) force is needed to stop the robot, which can be directly interpreted by eq.(23) or (24). The purpose of power assistance for the caregiver is achieved. In addition, Fig. 9 indicates that a slow and big pushing force occurs at the start to move the robot, while there is no such phenomenon in Fig. 10. This can be explained as follows. The parameter M_x, the virtual mass coefficient, is set to be 15.4[kg] in Fig.9 and M_x is 7.0[kg] in Fig.10. Since mass is a metric of inertia, the more the inertia of an object is, the slower the object starts to move. But a too small M_x will make the system too sensitive to the exerted force. This will lead to the user fearful to use the robot.

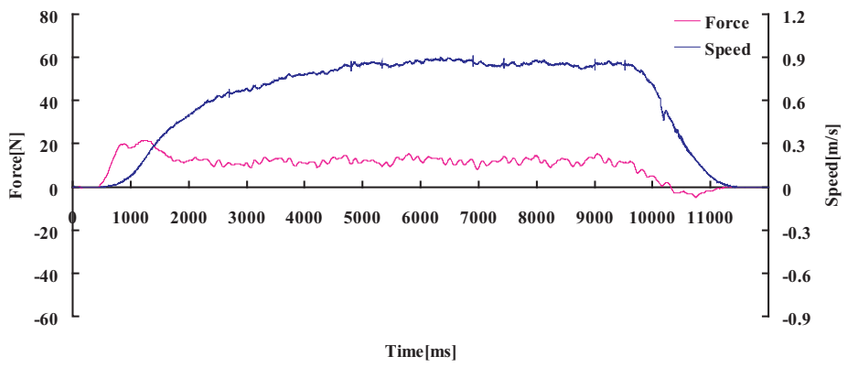

Fig. 9. Forward Experimental result with assistance (as $D_x = 14$ and $\tau_x = 1.1$)

5.3 Forward experiments with power assistance as D_x=9, 19[N·s/m]

The result of power assistance experiment with $D_x = 9$[N·s/m] and $\tau_x = 0.5$[s] ($M_x = 4.5$[kg]) is shown in Fig. 11. The result shows that the pushing force is about 7[N] when the walking speed is about 0.9[m/s]. The experiment result with $D_x = 19$[N·s/m] and $\tau_x = 0.5$[s] ($M_x = 9.5$[kg]) is shown in Fig. 12. The pushing force is about 17[N] as the walking speed is about 0.9[m/s]. Same as the above, these results demonstrate that the pushing force (the

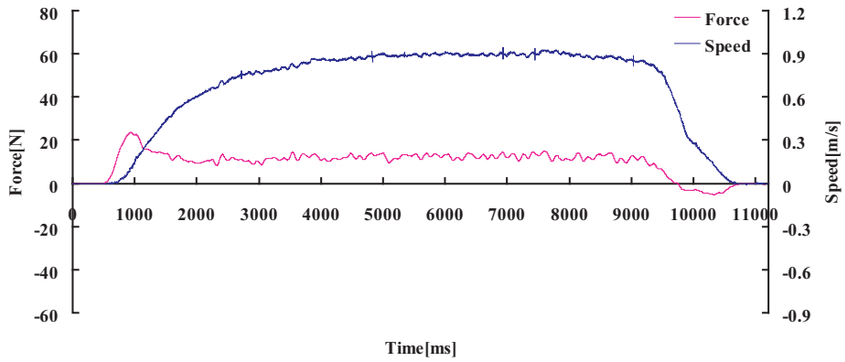

Fig. 10. Forward experimental result with assistance (as $D_x = 14$ and $\tau_x = 0.5$)

user's burden) is well controlled by the admittance based controller. In Fig. 10 there occurs a comparatively big force for starting to move the robot. As aforementioned, this is caused by a relatively big mass coefficient M_x. How to optimally select the two parameters is one of our future tasks.

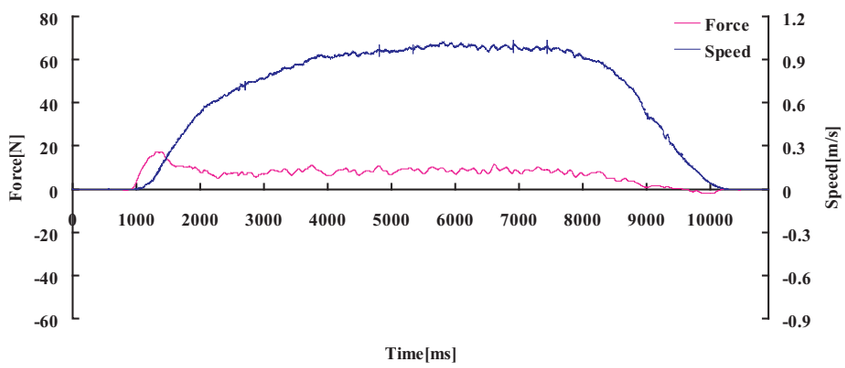

Fig. 11. Forward experimental result with assistance (as $D_x = 9$ and $\tau_x = 0.5$)

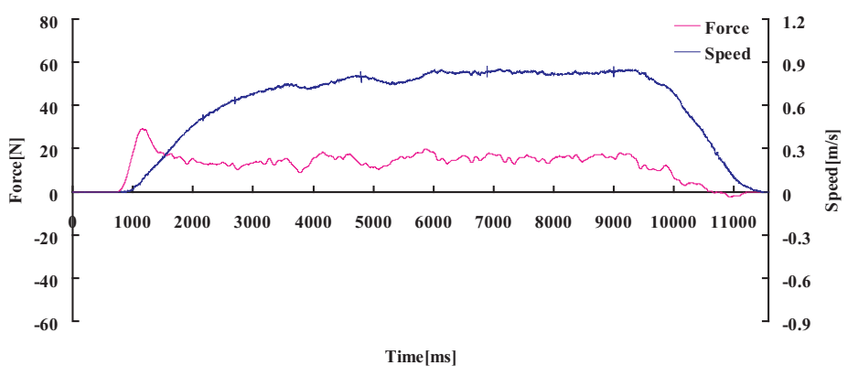

Fig. 12. Forward experimental result with assistance (as $D_x = 19$ and $\tau_x = 0.5$)

5.4 Lateral experiments without power assistance

We turn off the motor drivers and do the experiment without power assistance. In this case, the motors are in free state. From the the result shown in Fig. 13, we can find:

1. to start to move the robot, a big pushing force as large as 40[N] is needed.
2. in steady state, the pushing force is about 22[N].
3. to stop the robot, a negative (pulling) force is needed.
4. the user's walking speed is about 0.6[m/s].

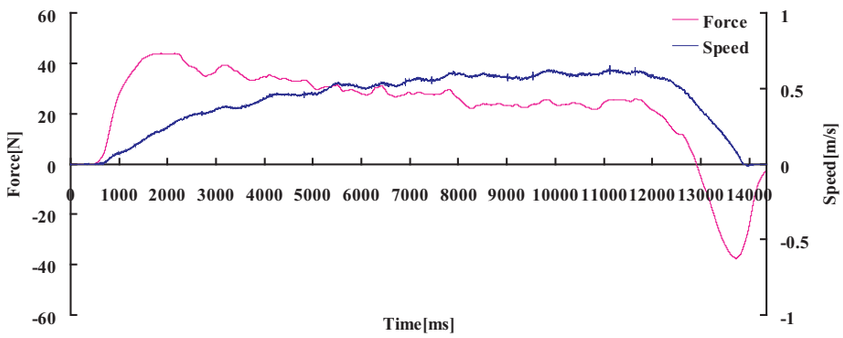

Fig. 13. Lateral experimental result without assistance

5.5 Lateral experiments with power assistance as $D_y = 18$[N·s/m]

In this case, we try to halve the user's burden with power assistance to about 11[N]. Since the user's walking speed is about 0.6[m/s], according to eq.(24) we set $D_y = F_{ys}/V_{ys} = 18$[N·s/m].

Fig. 14 shows the experimental results with $\tau_y = 0.5$[s] ($M_y = 9$[kg]). The results show that the pushing force is reduced to about 11[N] from about 22[N] when the steady walking speed is about 0.6[m/s] as we planned, and a very small pulling (negative) force appeared to stop the robot. The purpose of power assistance for the caregiver is achieved.

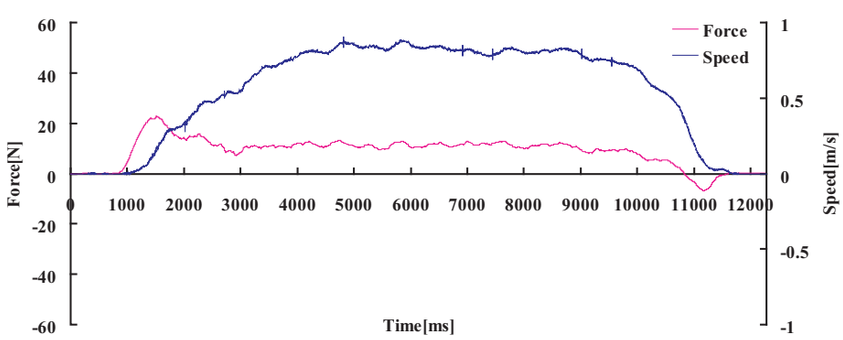

Fig. 14. Lateral experimental result with assistance (as $D_y = 14$ and $\tau_x = 0.5$)

5.6 Turning-on-the-spot experiment without power assistance

We switch off the motor drivers and do the experiment without power assistance. In this case, the motors are in free state. From the the result shown in Fig. 15, we can find:

1. to start to move the robot, a big pushing torque as large as 19[Nm] is needed.
2. in steady state, the pushing torque is about 10[Nm].
3. to stop the robot, a negative (pulling) torque is needed.
4. the user's walking speed is about 0.8[rad/s].

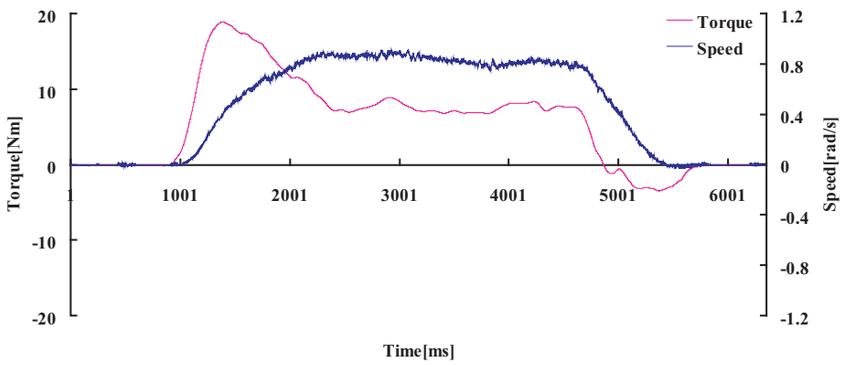

Fig. 15. Turning-on-the-spot experimental result without assistance

5.7 Turning-on-the-spot experiments with power assistance as $D_z = 6$[Nm·s/rad]

In this case, we also try to halve the user's burden with power assistance to about 5[Nm]. Since the user's walking speed is about 0.8[rad/s], according to eq.(24) we set $D_z = F_{zs}/V_{zs} = 6$[Nm·s/rad].

Fig. 16 shows the experimental results with $\tau_z = 0.5$[s] ($I_z = 9$[kg m^2]). The results show that the pushing torque is reduced to about 11[Nm] from about 22[Nm] when the steady walking speed is about 0.6[rad/s] as we planned, and no pulling (negative) torque is needed to stop the robot, which can be directly interpreted by eq.(23). The purpose of power assistance for the caregiver is achieved.

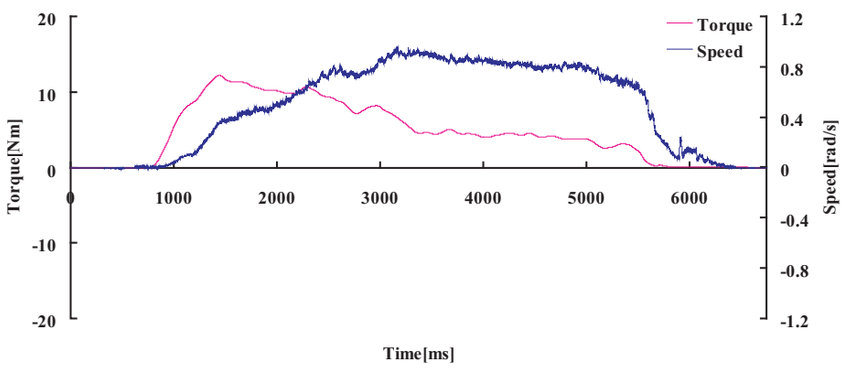

Fig. 16. Turning-on-the-spot experimental result with assistance (as $D_z = 6$ and $\tau_z = 0.5$)

6. Conclusions

In this research, we developed a new type of omnidirectional mobile robot that not only can fulfill the walking support or walking rehabilitation as the elderly or the disabled walks while holding the robot handle, but also can realize the power assistance for a caregiver when he/she pushes the robot to move while the elderly or the disabled is sitting in the seat. The omnidirectional mobility of the robot is analyzed, and an admittance based human-machine interaction controller is introduced for power assistance. The experimental results show that the pushing force is reduced and well controlled as we planned and the purpose of walking support and power assistance is achieved.

7. References

Dicianno, B. E., Spaeth, D. M. & Rory A. Cooper, e. a. (2007). Force control strategies while driving electric powered wheelchairs with isometric and movement-sensing joysticks, *IEEE Transactions on Neural Systems and Rehabilitation Engineering* Vol.15(No.1): 144–150.

Graf, B., Hans, M. & Schraft, R. D. (2004). Care-o-bot ii.development of a next generation robotic home assistant, *Autonomous Robots* Vol.16(No.2): 193–205.

Han, F., Yamada, T., Watanabe, K., Kiguchi, K. & Izumi, K. (2000). Construction of an omnidirectional mobile robot platform based on active dual-wheel caster mechanisms and development of a control simulator, *Journal of Intelligent and Robotics Systems* Vol.29(No.3): 257–275.

Kakimoto, A., Matsuda, H. & Sekiguchi, Y. (1997). Development of power-assisted attendant-propelled wheelchair, *Proc. of 19th Annual International Conference of the IEEE Engineering in Medicine and Biology Society*, pp. 1875–1876.

Lacey, G. & Dawson-Howe, K. M. (1998). The application of robotics to a mobility aid for the elderly blind, *Robotics and Autonomous Systems* Vol.23(No.4): 245–252.

Miyata, J., Kaida, Y. & Murakami, T. (2008). $v-\dot{\phi}$ coordinate-based power-assist control of electric wheelchair for a caregiver, *IEEE Transactions on Industrial Electronics* Vol.55(No.6): 2517–2524.

Nemoto, Y. & M. Fujie, e. a. (1998). Power-assisted walking support system for elderly, *Proc. of the 20th Annual International Conference of the IEEE Engineering in Medicine and Biology Society*, pp. 2693–2695.

Newman, W. (1992). Stability and performance limits of interaction controllers, *Transactions of the ASME, Journal of Dynamics Systems, Measurement, and Control* Vol.114(No.4): 563–570.

S. Dubowsky, e. a. (2000). Pamm-a robotic aid to the elderly for mobility assistance and monitoring: A "helping-hand" for the elderly, *Proc. of 2000 IEEE International Conference on Robotics and Automation*, pp. 570–576.

Ulrich, I. & Borenstein, J. (2001). The guidecane - applying mobile robot technologies to assist the visually impaired, *IEEE Transactions on System, Man, and Cybernetics-Part A: Systems and Humans* Vol. 31(No. 2): 131–136.

Wada, M. & Mori, S. (1996). Holonomic and omnidirectional vehicle with conventional tires, *Proc. of 1996 IEEE International Conference on Robotics and Automation*, pp. 3671–3676.

Yanco, H. A. (1998). Integrating robotic research: A survey of robotic wheelchair development, *AAAI Spring Symposium on Integrating Robotic Research*, Stanford University, CA.

Yu, H., Spenko, M. & Dubowsky, S. (2003). An adaptive shared control system for an intelligent mobility aid for the elderly, *Autonomous Robots* Vol.15(No.1): 53–66.

Yu, H., Spenko, M. & Dubowsky, S. (2004). Construction of an omnidirectional mobile robot platform based on active dual-wheel caster mechanisms and development of a control simulator, *Transactions of the ASME, Journal of Mechanical Design* Vol.126(No.8): 822–829.

Zhu, C., Oda, M., Suzuki, M., Luo, X., Watanabe, H. & Yan, Y. (2010). A new type of omnidirectional wheelchair robot for walking support and power assistance, *Proc. of 2010 IEEE International Conference on Intelligent Robots and Systems*, pp. 6028–6033.

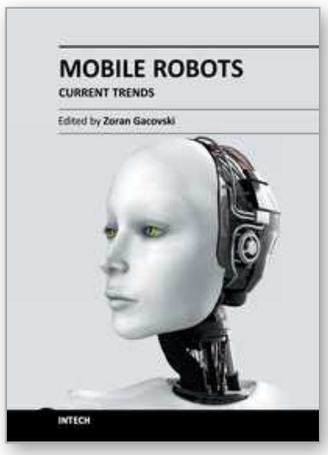

Mobile Robots - Current Trends

Edited by Dr. Zoran Gacovski

ISBN 978-953-307-716-1
Hard cover, 402 pages
Publisher InTech
Published online 26, October, 2011
Published in print edition October, 2011

This book consists of 18 chapters divided in four sections: Robots for Educational Purposes, Health-Care and Medical Robots, Hardware - State of the Art, and Localization and Navigation. In the first section, there are four chapters covering autonomous mobile robot Emmy III, KCLBOT - mobile nonholonomic robot, and general overview of educational mobile robots. In the second section, the following themes are covered: walking support robots, control system for wheelchairs, leg-wheel mechanism as a mobile platform, micro mobile robot for abdominal use, and the influence of the robot size in the psychological treatment. In the third section, there are chapters about I2C bus system, vertical displacement service robots, quadruped robots - kinematics and dynamics model and Epi.q (hybrid) robots. Finally, in the last section, the following topics are covered: skid-steered vehicles, robotic exploration (new place recognition), omnidirectional mobile robots, ball-wheel mobile robots, and planetary wheeled mobile robots.

InTech Europe
University Campus STeP Ri
Slavka Krautzeka 83/A
51000 Rijeka, Croatia
Phone: +385 (51) 770 447
Fax: +385 (51) 686 166
www.intechopen.com

InTech China
Unit 405, Office Block, Hotel Equatorial Shanghai
No.65, Yan An Road (West), Shanghai, 200040, China
中国上海市延安西路65号上海国际贵都大饭店办公楼405单元
Phone: +86-21-62489820
Fax: +86-21-62489821

IntechOpen